

# Superelasticity Behaviour of NiTi Actuator at Different Strain Rates

Sivasanghari Karunakaran\*, Dayang Laila Abang Abdul Majid, Husam Yahya Imran

*Department of Aerospace Engineering, Faculty of Engineering, Universiti Putra Malaysia, 43400 Serdang, Selangor, Malaysia*

## ABSTRACT

A small compact shape memory alloy actuator wire can generate large forces repeatedly and have found significant potential in aerospace components. Thermomechanical characterization of actuator wire under tensile loading can cause extreme sensitivity of the SMA material response, thus affect the performances of SMA. Previously, most research were focused on the effect of compositions and manufacturing parameters on the performances of SMA. Nonetheless, several factors like strain rate, activation temperature and activation time can potentially affect the performance of SMA. This experimental study investigated the strain rate effect on the superelasticity behaviour of the NiTi actuator with diameter of 0.31mm at a constant activation temperature of 70°C. Instron 3366 Universal Testing Machine (UTS) with a 5 kN load cell, which was mounted with heat control chamber, was used to apply uniaxial tension to the NiTi wire. The test underwent loading and unloading process at three different strain rates of 0.04 mm/min, 0.2 mm/min and 1.0 mm/min, respectively. The results showed that the phase transformation stresses and stress during the transformation phase increased with increasing strain rate. Hysteresis loop increased gradually with strain rate but showed significant reduction at higher strain rate. Overall, this study successfully highlighted the potential influences of strain rate on the possible use of SMA actuator in large force generation applications.

**Keywords:** Strain rate, Phase transformation stress, Hysteresis response, NiTi wire, Shape memory alloy

## I. INTRODUCTION

Nickel titanium (NiTi) alloy is a smart material that is classified in the family of shape memory alloy (SMA). Due to reliability and reproducibility of its response when stimulated with stress or temperature [1], it has received a great interest for use in actuation and auxiliary control [2], including in the aerospace fields. The two most prominent functional properties of SMA that make it as a unique material are super elasticity (SE) and shape memory effect (SME) [3,4]. SE is the ability of the SMA to revert to its original shape after deformation while SME is the ability of the SMA to revert to its original shape after deformation through heating [3]. Both of these functional properties are

exhibited due to reversible phase transformation between martensite phase and austenite phase [4,5].

In general, superelasticity is a functional property of SMA that refers to the elastic response exhibited by SMA when exposed to external applied stress. It is associated with the transformation to detwinned martensite during the loading and the reversal austenite upon unloading [6]. An isothermal superelastic loading and unloading path is illustrated in Figure 1. The point 1-2 represents the elastic deformation of austenite phase and point 2-3 is the phase transformation from austenite to martensite. In this phase, the detwinning of martensite starts at point 2 and results in fully detwinned martensite at point 3. The continuous application of load will cause elastics deformation of the detwinned martensite at point 3-4. Point 4-5 corresponds

to reverse transformation in which the elastic deformation of martensite phase takes place upon unloading. The point 5-6 represents austenite transformation upon subsequent

unloading. In this phase, the material is reverting to austenite and the transformation strain is recovered at point 6-1.

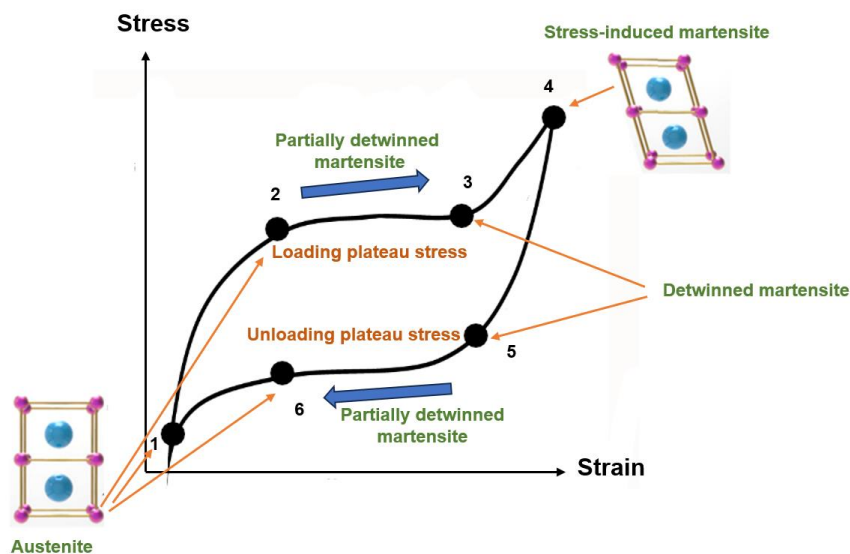


Figure 1 Illustration on the superelasticity characterization of SMA [7]

Today, the aerospace field has been actively seeking new SMA integrated technology for novel solutions and applications due to the ability of SMA to produce greater displacement and energy density. For instance, the SMA is used in propulsion system and structural configuration on aircraft for wing morphing [6], and flapping wing in micro aerial vehicles [7]. In the Smart Wing Program, the SMA actuator replaces traditional electromechanical actuator in lifting devices to optimize its performances by providing power density [6-8]. On the other hand, the Smart Aircraft and Marine Propulsion System (SAMPSON) successfully demonstrated the adaptation of SMA actuator in providing the actuation to change the orientation and the geometry of gas turbine inlets and propulsion devices by employing shape memory effect [9]. Furthermore, Variable Geometry Chevron (VGC) integrated SMA in aerodynamic devices has demonstrated minimum deflection flow, reduced noise and also increased efficiency during cruising [10,11]. For similar application, Hartl et al. [12] conducted training and characterization on actuation properties of two different compositions of SMA active beam actuator to reduce the jet engine noise while maintaining the efficiency during cruising. Another application related to SMA actuator is the experimental Morphing Laminar Wing (MLW), which employed SMA wire to improve the laminar flow regime on wing extrudes and thus achieved less fuel consumptions [6,13].

Researcher in recent years have conducted extensive amount of research on the thermomechanical behaviour of NiTi wire using tensile testing due its capability to recover large strain after deformation [14,15]. As a stress and temperature sensitivity material, NiTi SMA exhibits stress induced behaviour when exposed to variation of strain amplitude and activation temperature. However, limited research has been conducted on the investigation of the

influence of strain rate at the activation temperature on the superelasticity behaviour of NiTi wire. The superelasticity behaviour of NiTi wire is dependent on the mechanical training parameters like strain rate, activation temperature, activation time, size of actuator and strain amplitude [16,17]. Most of the previous studies investigate the effect of strain rate on the evolution of microstructure evolution, mechanism of thermodynamic and the composition of the SMA material [18-20]. The range of strain rates adopted in these previous research work was between  $10^{-4}$  mm/s to 2 mm/s. Unfortunately, all results under different strain rate were based on microscopic measurements. Observation on the macroscopic stress-strain responses of the SMA at activation temperature was not reported, probably due to the experimental difficulty to get these results at constant temperature. Hence, most of the superelasticity behaviour of NiTi wire is often misinterpreted as it is complex and non-linear. This leads to the inaccurate extraction of the thermomechanical data to characterize the application of NiTi wire. In most practical applications, the engineering working environment is rasing for the actuators and the structures due the exposure to dynamic loading conditions [20].

In view of this, the present work aims to investigate effect of the strain rate on the superelasticity behaviour of the NiTi wire under tensile test at activation temperature of  $70^{\circ}\text{C}$ . In this study, the activation temperature of  $70^{\circ}\text{C}$  is defined as the minimum temperature required for the NiTi wire to induce its superelasticity behaviour. The main goal of this work is the experimental determination of the thermomechanical properties of SMA such as phase transformation stress and stress during phase transformation in the analysis of ideal path for phase transformation in the analysis of engineering applications.

The hysteresis response of NiTi wire is also addressed for the actuation capabilities.

## II. MATERIAL AND METHODOLOGY

### 2.1 Materials

The SMA used in this study is nickel titanium (NiTi) made by Dynalloy, USA company with the trade name of Flexinol actuator wire [21]. The SMA is nearly equatomic composition and its diameter is 0.31 mm with maximum allowable safe stress of 172 MPa. The technical properties of the SMA wire are listed in Table 1.

Table 1 Properties of nickel titanium wires [21]

Parameters	Values
Composition	50% Ni, 50% Ti
Diameter	0.31 mm
Melting point	1300°C
Specific heat	0.2 cal/g * °C
Density	6.45 g/cm <sup>3</sup>
Latent heat of transformation	5.78 cal/g
Thermal conductivity	0.18 W/cm * °C
Poisson ratio	0.33
Activation Temperature	70°C

### 2.2 Methodology

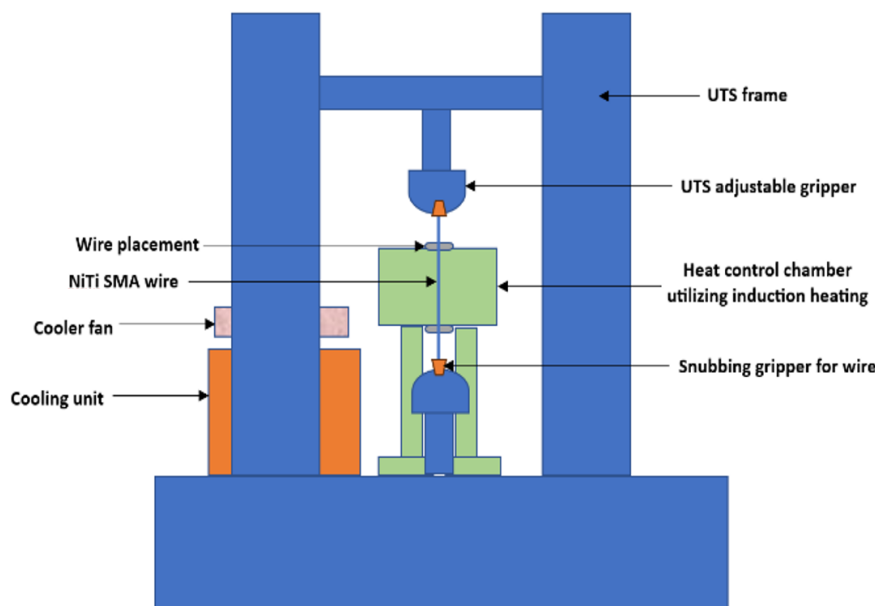
The experiments for characterising the superelastic behaviour of the NiTi SMA wire were conducted using the equipment shown in Figure 2(a). The tensile test system consisted of an Instron 3366 Universal Testing Machine (UTS). The loading cell used for the tensile test was 5 kN

to ensure an accurate low-level loading and displacement measurements. A heat control chamber that was comprised of induction heating mechanism was mounted to the UTS machine for the heating of the wire specimens. Each of wire specimen was placed inside the chamber and inserted through the induction coil and clamped via a snubbing gripper, which was clamped to the UTS gripper. The wire specimen was enclosed by the contactless induction coil to ensure uniform heat distribution throughout the specimen and to prevent any damages to the specimen. The strain of the NiTi wire was obtained from crosshead displacement that was reported by the UTS control software.

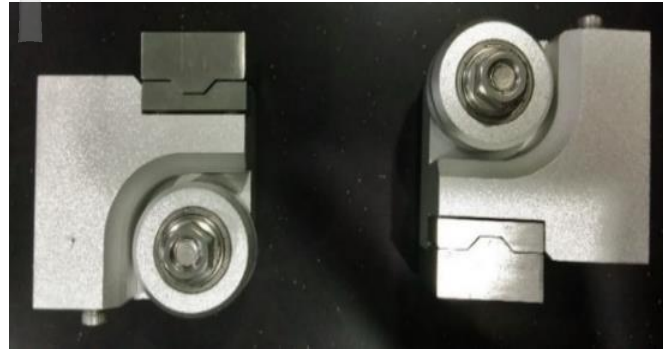
A series of loading (tensile) and also unloading (compression) tests were conducted using the test system in Figure 2(a) to obtain basic superelastic characteristics of the NiTi wire including phase transformation stresses, stress during the phase transformation (plateau region), hysteresis and the relationship of stress-strain curves of the NiTi wires. Each loading and unloading were performed at a constant temperature of 70°C

at a strain rate of 0.04 mm/min as recommended in ASTM F2516 standard [22]. Before the test, a pretension of approximately 0.1 N was applied manually at constant low speed to tighten the Flexinol wire. Then, the displacement and load cell were calibrated and set to zero. The free length of the specimens between both the end of the snubbing grips was 100 mm for the tests. In short, the steps taken for the tensile test were:

- heating the NiTi wire at 70°C for two minutes in the absence of stress to keep the temperature constant for loading and unloading tests
- for the loading process, the wire was pulled to force level 172 MPa (12.5 N) at strain rate of 0.04 mm/min
- for the unloading process, the wire was compressed to zero load with the same strain rate



(a)



(b)

Figure 2 (a) Schematic setup for induction heated actuated NiTi wire mounted on the tensile test; (b) Snubbing grips for wire tests

The force and displacement reading were recorded by the UTS control Bluehill Universal software. The loading and the unloading process were then repeated for other sets of strain rate, which were 0.2 mm/min and 1.0 mm/min, respectively. Each complete cycle was repeated for three

times. The temperature was monitored and also controlled using a specially developed user interface (UI) through the temperature profile connected by Bluetooth device in the chamber. The overall methodology of the present study is illustrated in the technical flowchart in Figure 3.

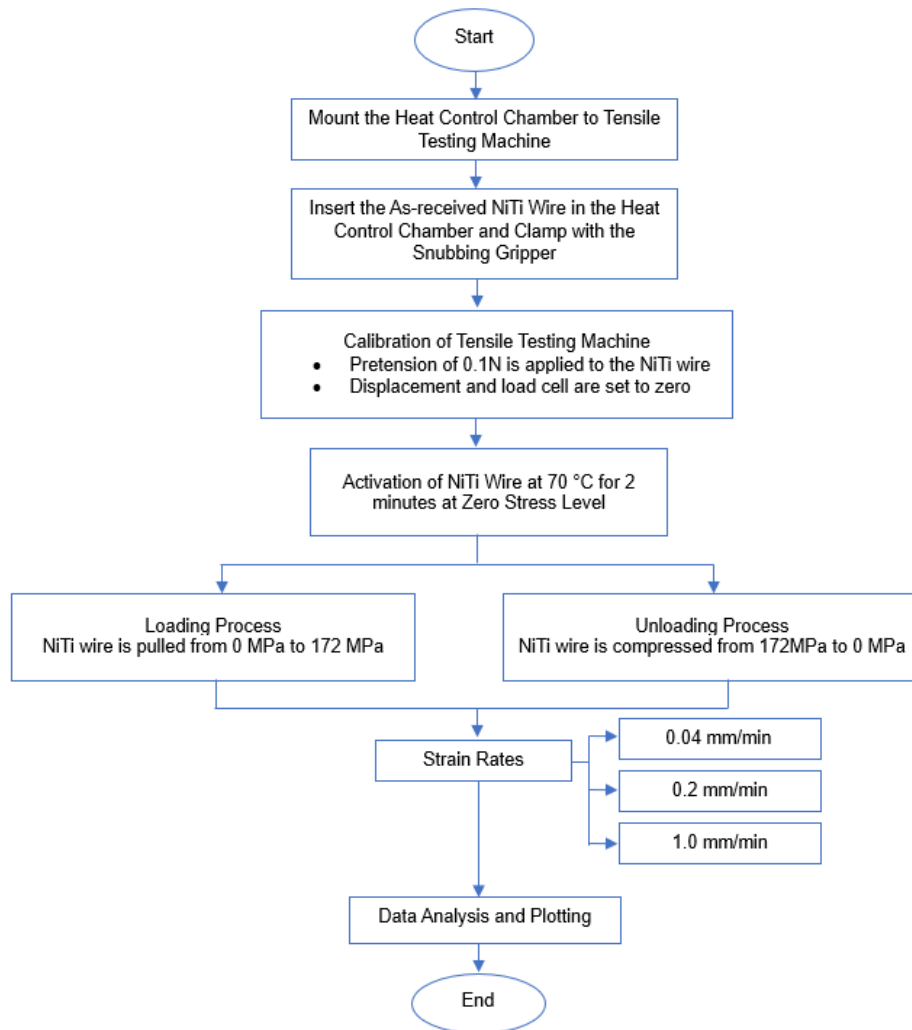


Figure 3 Technical flowchart of the research work

### III. RESULTS AND DISCUSSION

#### Phase Transformation Stress at Different Strain Rates

Figure 4 shows the relationship between the stress amplitude and strain response when the strain rate increases at activation temperature of 70°C. It clearly shows that there is a significant upward shift in stress amplitude, which indicates that the phase transformation stress increasing with increasing strain rate. On the other hand, the left shift in strain response shows that the stress

during phase transformation is increased with increasing strain rate. The similar flag shape loops are observed for all the strain rates and this implies that the NiTi wires had the same crystallographic orientation, which represents the superelasticity deformation. This means that the wire underwent large inelastic deformation during loading process and recovered its shape after unloading process. This also implies that the dissipated latent heat to the surrounding during the loading and unloading test were sufficient for the transformation to occur.

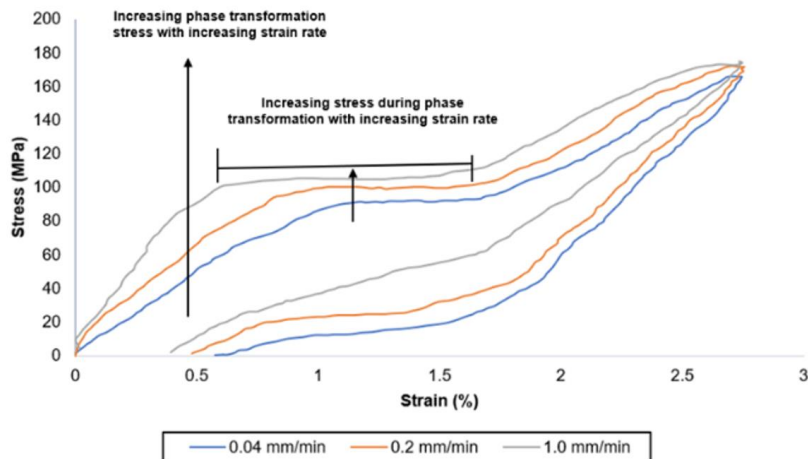


Figure 4 Superelasticity behaviour of NiTi wire at different strain rates

The derivation of thermomechanical parameters of the NiTi wire such as the phase transformation stress and stresses during the phase transformation during loading and unloading region are illustrated in Figure 4 to Figure 6. The four phase transformation stresses including stress at martensite start,  $\sigma_{Ms}$ , stress at martensite finish,  $\sigma_{Mf}$ , stress at austenite start,  $\sigma_{As}$  and stress at austenite finish,  $\sigma_{Af}$ , were determined through the dotted black line passing through both the plateau lines (forward and reverse phase) and intersect at the y-axis, which was represented by stress

quantity. On the other hand, the stresses during the phase transformation region were determined through horizontal dotted green line passing through the surface of plateau length of the graph. The stress value during the phase transformation from austenite to martensite phase is representing the forward transformation while the region from martensite to austenite is represented by reverse transformation. All thermomechanical parameters derived from Figure 5 to Figure 7 are tabulated in Table 2.

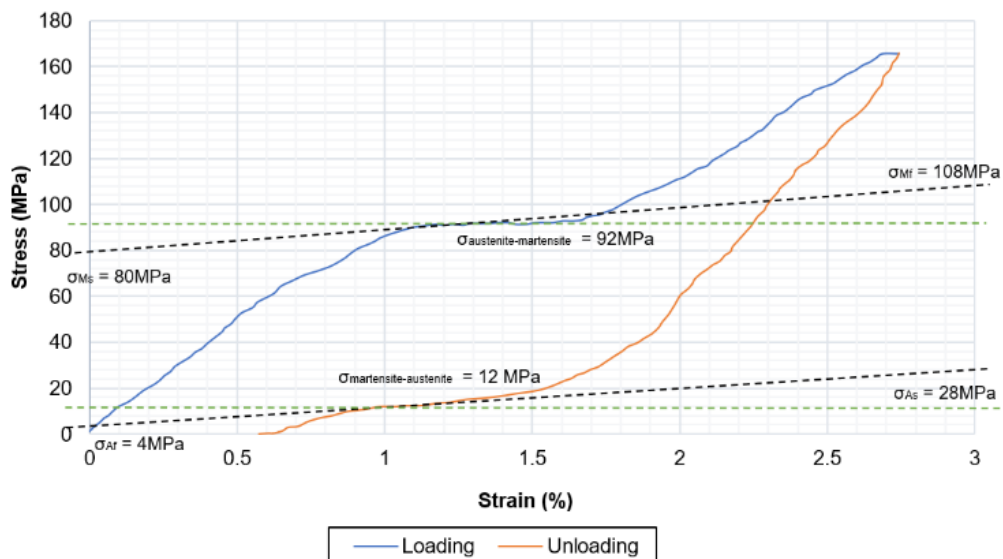


Figure 5 Derivation of parameters of NiTi wire at strain rate of 0.04 mm/min

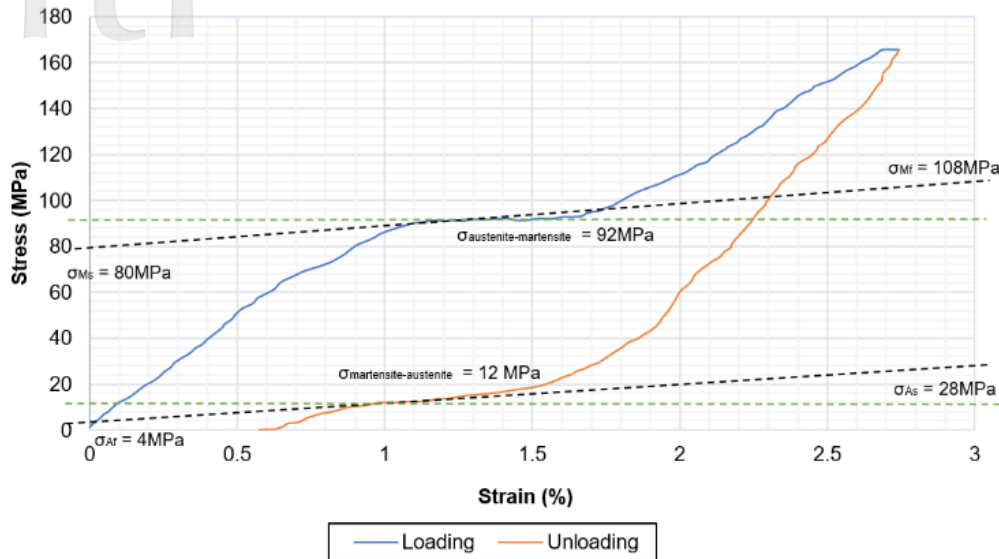


Figure 6 Derivation of parameters of NiTi wire at strain rate of 0.2 mm/min

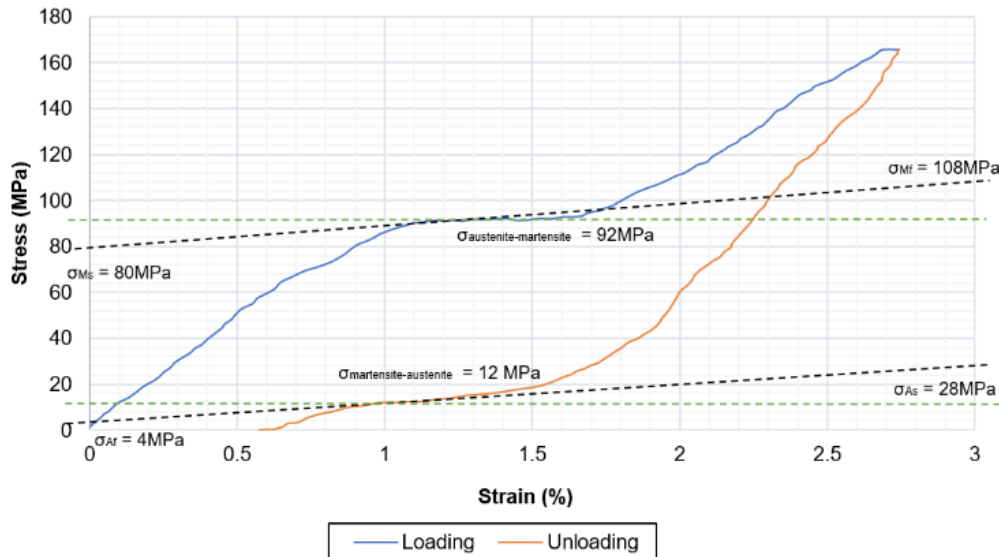


Figure 7 Derivation of parameters of NiTi wire at strain rate of 1 mm/min

Table 2 outlines that all the four phase transformation stress increases with increasing strain rate. Increasing the strain rate appeared to increase both forward and reverse transformation stresses, as well as elastic storage energy.

Table 2 Phase transformation stress of the NiTi wire

Strain rate (mm/min)	Phase Transformation Stresses (MPa)					
	$\sigma_{Ms}$	$\sigma_{Mf}$	$\sigma_{As}$	$\sigma_{Af}$	$\sigma_{A-M}$	$\sigma_{M-A}$
0.04	80	108	28	4	92	12
0.20	92	112	48	8	100	22
1.00	100	120	80	28	104	52

Therefore, more energy was needed for the microstructure to rearrange itself, causing the internal stress that being built up to rise because part of the transformation heat was left in the wire. This was because heat exchange rate between the wire and the surrounding was affected by temperature rise due to increasing strain rate [2]. Although this study investigated the superelasticity of NiTi wire at a constant activation temperature, the presence of different strain rates also influenced the heat energy generated during the transformation, hence affecting the phase transformation stress as well as the forward and reverse transformation stresses. When the loading was applied continuously to the wire, generated heat energy during phase transformation was released to the surrounding sufficiently [23]. The increase in strain rate further increased the amount of heat generated. This led to the rise in wire temperature during



the loading and unloading process, causing increase in the transformation rate [24]. To be more specific, the forward martensitic transformation stress was greater than that for the reverse martensitic transformation. Nonetheless, both increased with increasing strain rate. These phenomena represented by the plateau length as shown in Figure 4 to Figure 6. On the whole, this can be taken to indicate that more heat energy will be generated with increasing strain rate and more time will be needed for the forward and reverse martensite orientation to occur.

Superelastic hysteresis in this study is defined as the total heat energy dissipated (internal stress) in the wire in one cycle of testing, loading and unloading path [25]. This region is represented by the area under the graph, which is the enclosed area during the loading and unloading process [26]. The flag shape of the hysteresis loop for all different strains was essentially similar. However, for each strain rate, the amount of heat dissipated was different. Besides that, the hysteresis loops narrowed and shifted upwards as the strain rate was increased. This indicates that the transformation point had shifted to the higher stress as discussed in the previous section.

In Table 3, the hysteresis of the wire increases from  $138.7 \text{ J/m}^3$  to  $146.7 \text{ J/m}^3$  for  $0.04 \text{ mm/min}$  and  $0.2 \text{ mm/min}$  strain rate, respectively. However, the hysteresis notably drops to  $139.3 \text{ J/m}^3$  at strain rate of  $1.0 \text{ mm/min}$ . This is due to the formation of forward and reverse transformation that are not able to cope with the higher strain rate. This indicates that, at higher strain rate, the martensite transformation does not provide enough deformation, thus leads to austenitic phase transformation due to the dislocation drags effect [2]. This can be observed in the reverse martensite transformation in which the dislocation drag mechanism reduces the plateau length of the transformation phase causing significant reduction in the hysteresis value. Here, a small percentage of plastic deformation of austenite occurs with minor reverse martensite transformation and this deformation takes place before the interface of the phase transformation start to rearrange itself. Besides that, strain rate is also associated with heat energy dissipation. The temperature of wire specimen increases with increasing strain rate due to the latent heat of transformation which lead to self-heating of the specimen during test. Therefore, the hysteresis loop narrowed with increasing strain is due to the self-heating of wire [27].

Table 3 Hysteresis of NiTi Flexinol wire

Strain rate (mm/min)	Hysteresis ( $\text{J/m}^3$ )
0.04	138.7
0.20	146.7
1.00	139.3

Herein, the investigation of stress-strain curve of the SMA wire subjected to the loading and unloading cycle reveals that the variation of continuous loading and increment of strain rates will significantly influence the superelasticity behaviour of the SMA wire at constant

activation temperature. DesRoches et al. [28] investigated the effect of strain rate on NiTi wires with the loading frequencies of  $0.025$ ,  $0.5$  and  $1.0 \text{ Hz}$  at constant amplitude. It is concluded that the forward and reverse transformation stresses increase with the increasing frequency while the hysteresis decreases. On the other hand, Dolce et al. [29] investigated the strain effect on NiTi wires in austenite conditions and concluded that the yield stress increases with increasing strain rate while the hysteresis loop narrows and shifts upwards. Humbeeck et al. [30] in their investigation concluded that the strain rate effect on the change in hysteresis is attributed by the exothermic and endothermic transformation. The study conducted by Tobushi et al. [23] on the influence of strain rate on NiTi properties concluded that the phase transformation stress and recoverable strain energy were strongly dependent on the range of strain rate. It can be noted that the published work on the strain rate effect on the NiTi superelastic behaviour varies depending on the range of strain rate as well as the range of activation temperature applied in the investigation. This further can be verified through the experimental data obtained in this investigation.

Based on the above discussion, it can be concluded that different strain rates exhibit different mechanical properties in terms of phase transformation stress and hysteresis. Inappropriate selection of strain rate can alter the mechanical properties of the material thus lead to plastic deformation and inhibit the use of the SMA material in desired application. Besides that, strain rate selection is also important to train the SMA material for specific application. Therefore, it is very important to understand the effect of wide range of strain rate on the thermomechanical properties of the NiTi wires, as well as their phase transformation stress and hysteresis, in order to assess the capability of SMA application in actuation devices [31] and components in structural system specifically in the functional approach such as energy dissipation, recentring, elimination of residual deformation and also displacement sensors.

#### IV. CONCLUSIONS

In this study, effects of strain rate on superelasticity behaviour of NiTi SMA wire was investigated and the following conclusions can be drawn. Firstly, the phase transformation stress and also the stress during phase transformation have varied depending on the strain rate. The higher the strain rate, the higher the value of these superelasticity properties of NiTi wire at constant activation temperature of  $70^\circ\text{C}$ . Secondly, as the strain rate climbs, the phase transformation stress increases due to the gradual growth of the dissipated heat energy, causing temperature variation of wire. Increasing the strain rate further influences the temperature of wire, thus bring increase in both forward and reverse martensitic transformation. Last but not the least, the hysteresis loop gradually increases with increasing strain rate. However, at higher strain rate, the hysteresis shows significant reduction due to the dislocation drag effect.

Moving forward, among the proposed future research direction include experimental studies on the performance

of NiTi wire at wider strain rates, investigation on the microstructure of NiTi wire at different strain rate and improvements on the thermomechanical behaviour of NiTi wire to take account of displacement or strain response for actuation application.

### ACKNOWLEDGMENTS

The authors would like to acknowledge the financial support from the Ministry of Higher Education under the Fundamental Research Grant Scheme (FRGS) with grant no. FRGS/1/2019/STG07/UPM/02/10.

### REFERENCES

- [1] Chien PY, Martins JNR, Walsh LJ, Peters OA, “Mechanical and metallurgical characterization of nickel-titanium wire types for rotary endodontic instrument manufacture,” *Materials*, Vol. 15, 2022, 8367.
- [2] Wang Z, Luo J, Kuang W, Jin M, Liu G, Jin X, Shen Y, “Strain rate effect on the thermomechanical behavior of NiTi shape memory alloys: a literature review.” *Metals*, Vol. 13, 2023, 58.
- [3] Zhou M, Li Y, Zhang C, Li S, Wu E, Li W, Li L, “The elastocaloric effect of Ni50.8Ti49.2 shape memory alloys,” *Journal of Physics D: Applied Physics*, Vol. 51, 2018, 135303.
- [4] Casagrande L, Menna C, Asprone D, Ferraioli M, Auricchio F, “Chapter 21—Buildings. in shape memory alloy engineering”, 2nd ed.; Concilio, A., Antonucci, V., Auricchio, F., Lecce, L., Sacco, E., Eds.; Butterworth-Heinemann: Boston, MA, USA, 2021, pp. 689-729.
- [5] Seo J, Hu JW, Kim KH, “Analytical investigation of the cyclic behavior of smart recentering t-stub components with superelastic SMA bolts,” *Metals*, Vol. 7, No. 10, 2017, 386.
- [6] Hartl DJ, Lagoudas DC, “Aerospace applications of shape memory alloys,” *Proceedings of the Institution of Mechanical Engineers, Part G: Journal of Aerospace Engineering*, Vol. 221, No. 4, 2007, pp. 535-552.
- [7] Awang Jumat N, Ogunwa TT, Abdullah EJ, Chahl J, Romli FI, Abdul Majid DL, “Flapping actuation using temperature feedback control of coated shape memory alloy actuators,” *Microsystem Technologies*, Vol. 27, 2021, pp. 3299-3311.
- [8] Carman G, Inman D, Kudva J, Leo DJ, “Memorial article for Ephraim Garcia,” *Smart Materials and Structures*, Vol. 24, No. 11, 2015, 110201
- [9] Costanza G, Tata ME, “Shape memory alloys for aerospace, recent development and new applications: a short review,” *Materials*, Vol. 13, No. 8, 2020, 1856.
- [10] Hartl D, Lagoudas DC, “Characterization and 3-D modeling of Ni60Ti SMA for actuation of a variable geometry jet engine chevron,” *Proceedings of SPIE*, 2007.
- [11] Kim MS, Heo JK, Rodrigue H, Lee HT, Pané S, Han MW, Ahn SH, “Shape memory alloy (SMA) actuators: The role of material, form, and scaling effects,” *Advanced Material*, Vol. 35, No. 33, 2023, 2208517.
- [12] Hartl DJ, Lagoudas DC, Calkins FT, Mabe JH, “Use of a Ni60Ti shape memory alloy for active jet engine chevron application: I. Thermomechanical characterization,” *Smart Materials and Structures*, Vol. 19, No. 1, 2010, 015020
- [13] Brailovski V, Terriault P, Georges T, Coutu D, “SMA Actuators for morphing wings,” *Physic Procedia*, Vol. 10, 2010, pp. 197-203.
- [14] Melton KN, Mercier O, “The mechanical properties of NiTi-based shape memory alloys,” *Acta Metallurgica*, Vol. 29, 1980, pp. 393-398.
- [15] Adler PH, Yu W, Pelton AR, Zadno R, Duerig TW, Barresi R, “On the tensile and torsional properties of pseudoelastic NiTi.” *Scripta Metallurgica et Materialia*, Vol. 24, 1990, pp. 943-970.
- [16] Soares GC, Rodrigues MCM, Santos LA, “Effects of temperature and strain rate on the mechanical behavior of a superelastic Niti wire,” *Proceedings of 71<sup>th</sup> ABM Annual Congress*, 2016.
- [17] Gall K, Tyber J, Brice V, Frick CP, Maier HJ, Morgan N, “Tensile deformation of NiTi wires,” *Journal of Biomedical Materials Research: Part A*, Vol. 75, No. 4, 2005, pp. 810-823.
- [18] Nnamchi P, Younes A, González S, “A review on shape memory metallic alloys and their critical stress for twinning,” *Intermetallics*, Vol. 105, 2019, pp. 61-78.
- [19] Šittner P, Sedlák P, Seiner H, Sedmák P, Pilch J, Delville R, Heller L, Kadeřávek L, “On the coupling between martensitic transformation and plasticity in NiTi: Experiments and continuum-based modelling,” *Progress Material Science*, Vol. 98, 2018, pp. 249-298.
- [20] Lin C, Wang Z, Yang X, Zhou H, “Experimental study on temperature effects on NiTi shape memory alloys under fatigue loading,” *Materials*, Vol. 13, No. 3, 2020.
- [21] DYNALLOY, Inc. (2023). Technical Characteristics of Flexinol [Actuator Wires]. Retrieved from <https://www.dynalloy.com/pdfs/TCF1140.pdf>
- [22] ASTM F2516 (2022) Standard Test Method for Tension Testing of Nickel-Titanium Superelastic Materials ASTM International, West Conshohocken, PA, USA
- [23] Tobushi H, Shimeno Y, Hachisuka T, Tanaka K, “Influence of strain rate on superelastic properties of TiNi shape memory alloy,” *Mechanic of Material*, Vol. 30, 1998, pp. 141-150.
- [24] Zhang X, Wang G, Luo B, Bland SN, Tan F, Zhao F, Zhao J, Sun C, Liu C, “Mechanical response of near-equiatomic NiTi alloy at dynamic high pressure and strain rate,” *Journal of Alloys and Compounds*, Vol. 731, 2018, pp. 569-576.
- [25] Hu JW, Noh MH, “Seismic response and evaluation of SDOF self-centering friction damping braces subjected to several earthquake ground motions,” *Advances in Materials Science and Engineering*, Vol. 2015, 2015, 397273.



- [26] Wang SW, Chuang SH, Wu CH, Hsu LH, Huang CM, "Study on static and dynamic aerodynamic characteristics of double delta wing at high angles of attack," *Journal of Aeronautics, Astronautics and Aviation*, Vol. 40, No. 3, 2008, pp. 151-162.
- [27] Dayananda GN, Rao SM, "Effect of strain rate on properties of superelastic NiTi thin wires," *Materials Science and Engineering A*, Vol. 486, 2008, pp 96-103
- [28] DesRoches R, McCormick J, Delemont M, "Cyclic properties of superelastic shape memory alloy wires and bars," *Journal of Structural Engineering*, Vol. 130, No. 1, 2004, pp. 38-46.
- [29] Dolce M, Cardone D, "Mechanical behaviour of shape memory alloys for seismic applications 2. Austenite NiTi wires subjected to tension," *International Journal of Mechanical Sciences*, Vol. 43, No. 11, 2001, pp. 2657-2677.
- [30] Humbeeck VJ, Delaey L, "The influence of strain-rate, amplitude and temperature on the hysteresis of a pseudoelastic Cu-Zn-Al single crystal," *Le Journal de Physique Colloques*, Vol. 42, No. C5, 1981, pp. 1007-1011.
- [31] Yang LJ, Kapri N, Waikhom R, Unnam NK, "Fabrication, aerodynamic measurement and performance evaluation of corrugated flapping wings," *Journal of Aeronautics, Astronautics and Aviation*, Vol. 53, 2021, pp. 83-94.